Analyst

ROYAL SOCIETY OF CHEMISTRY

PAPER

View Article Online
View Journal | View Issue

Cite this: *Analyst*, 2026, **151**, 1936

Novel H_2 colourimetric indicator for screening the activity of H_2-generating bacteria and measuring their total viable count (TVC)

Lauren McDonnell, Christopher O'Rourke, Michaella Watson and Andrew Mills *

A novel colourimetric H_2 indicator is described, comprising an intimate mixture of methylene blue, MB, and colloidal Pt particles, encapsulated in a polymer film and laminated between two thin sheets of low-density polyethylene. Upon exposure to H_2, the blue coloured indicator turns colourless, as the MB is reduced to *leuco* methylene blue, but is restored to its original blue colour by air. The indicator is easy to make, stable, and reproducible, and is used to detect the presence of both *gaseous* and *dissolved* H_2. The H_2 indicator is used to screen for H_2-generating bacteria, such as *Escherichia coli*, *Klebsiella aerogenes*, *Enterobacter cloacae*, and *Clostridium bifermentans*, under aerobic and anaerobic conditions. Here, the indicator is set in the bottom of a well plate containing the bacterium under test and its colour assessed by eye, or photographically. A value for the apparent absorbance, *A'*, of the indicator is obtained by digital colour analysis of its photograph and, for each bacterium, a series of reverse 'S' shaped *A' vs.* incubation time, *t*, profiles are generated using different inoculated growth medium samples, covering a wide total viable count (TVC) range, typically, 10^1–10^8 CFU mL^{-1}. Each profile has, at its half-way colour change point, an associated incubation time, t_{50}, and, for all the H_2 generating bacteria tested, the plot of log (TVC) *vs.* t_{50}, is a straight line. This calibration graph is the basis of a new microrespirometry method, H_2 μR-TVC, which compliments O_2 μR-TVC. The potential applications of the H_2 indicator are discussed briefly.

Received 19th November 2025,
Accepted 19th February 2026

DOI: 10.1039/d5an01221j

rsc.li/analyst

1. Introduction

There is growing interest in a H_2 economy, in which H_2 is used as fuel to produce electricity and heat, as a route to reduce significantly the emission of greenhouse gases and the associated deleterious climate change effects.[1] For a H_2 economy to be sustainable, H_2 production needs to utilise a renewable energy source, and a great deal of work is focused on using solar-driven, artificial photosynthetic systems to split water into H_2 and O_2.[2] However, H_2 can also be generated using photosynthetic bacteria, and by many non-photosynthetic bacteria, *via* various anaerobic, dark fermentation processes.[3,4] In either case, the bacteria are usually inexpensive and easy to produce and employ as the reducing agent, a renewable biomass with a high content of carbohydrate, such as glucose.[3,4] Dark fermentative, H_2-producing bacteria include *Enterobacter*, *Bacillus* and *Clostridium* sp., such as *Escherichia coli* (*E. coli*), *Bacillus mycoides* (*B. mycoides*) and *Clostridium bifermentans* (*C. bifermentans*), respectively. Although there are numerous pathways by which H_2 is produced from glucose by bacteria, the most desirable one involves the co-production of acetic acid and CO_2, *i.e.*,

$$\text{Glucose} \rightarrow 2\text{acetic acid} + 2CO_2 + 2H_2 \quad (1)$$

in which 2 moles of H_2 are produced for every 1 mole of glucose.[3] Interestingly, the ubiquitous bacterium, *E. coli*, is very effective at fermenting the production of H_2, producing 0.75 mole H_2 per mole of glucose.[5]

As there are numerous known, and also other, yet to be discovered, H_2-generating bacteria and algae, there is a real need for a simple, inexpensive system for screening microbial species for H_2 activity. This need is not easily addressed by the analytical methods that have been used in the past to assess microbial H_2 activity, such as gas chromatography and H_2 polarographic electrodes.[6–8] Of potential interest are colourimetric H_2 indicators, as inexpensive, easy to use alternatives to the traditional methods for monitoring levels of H_2 although, unfortunately, they are not usually able to measure *dissolved* H_2. Most of these indicators are based on metals, usually Pd,[9] metal oxides, such as WO_3 and MoO_3,[10,11] and dyes, such as tetrazolium and resazurin;[12,13] and are irreversibly reduced by

School of Chemistry and Chemical Engineering, Queens University Belfast, Stranmillis Road, Belfast, BT9 5AG, UK. E-mail: andrew.mills@qub.ac.uk

gaseous H_2, and cannot be readily regenerated and reused upon exposure to air. These indicators have been the subject of several excellent reviews,[14–18] and a representative selection of examples, particularly with regard to dye-based H_2 indicators, are listed in Table S1 in the SI. Note that there are very few examples of indicators that have been used to detect *dissolved* H_2, and all are solution-based and cannot be used in direct contact with bacteria and growth medium due to interference effects.[19]

A few of the H_2 *gas*, colourimetric indicators have been used to develop in a High-Throughput, H_2 Screening method (HTHS method) for assessing the H_2-generating activity of microbials.[6,19,20] For example, Schrader *et al.* has reported a high-throughput H_2 indicator-based system for assessing bacterial *gaseous* H_2 production activity comprising a 7 layer stacked system, with a lower 96-well plate containing the different H_2 producing bacteria under test and an upper, gas permeable membrane bottomed, 96-well plate containing the H_2 indicator *solution*.[19] The active agents in the indicator solution are, (i) an easily and *irreversibly* reduced tetrazolium dye, ST-1 and, (ii) a sulphonated, rhodium-containing, Wilkinson hydrogenation catalyst. After an incubation time of *ca.* 5 days, which in practice is much too long for a HTHS method, the stack is broken up and the absorbance of the indicator solutions (colour change: colourless to pale purple) measured using UV-Vis absorbance spectrophotometry. More recently, Koo *et al.* have reported an architecturally similar, but faster (*ca.* 10–30 min), stacked (7 layers), HTHS system for assessing bacterial H_2 production which utilises a WO_3/Pt *gaseous* H_2-sensitive indicator *film* (colour change: pale yellow to blue), which is placed above the H_2 generating bacteria under test in a 96-well plate.[20] Encouragingly, in this system, the stack doesn't need to be dismantled, as a CCD camera is placed above to measure the rate of change of colour of the indicator in each well; the response of the H_2 indicator is found to be non-linearly related to the rate of H_2 production. Unfortunately, both these HTHS systems are bulky and mechanically elaborate and, consequently, not easily scaled for manufacture as a commercial product.

In this paper, it is proposed that a simpler, faster screening system can be developed by, (i) placing a novel, colourimetric, *dissolved* H_2 indicator *film in* the growth medium with the bacterium under test, and (ii) monitoring its colour change *via* photography coupled with digital colour analysis, DCA.[21] Obviously, the response of a H_2-indicator to *dissolved* H_2, in such a system must be unaffected by, (i) the bacterium under test, (ii) their metabolites and (iii) the chemicals in the growth medium. In addition, the presence of the H_2 indicator in the growth medium must have no effect on the bacteria's growth kinetics. In addition, ideally the response of the H_2 indicator must be reversible, so that the indicator's colour can be restored upon exposure to air. None of the gaseous H_2 colourimetric indicators listed in Table S1, and those in the two HTHS systems described above, can address all of the above requirements. Instead, a new, very different, and ideally much less expensive, easier to make and use, colourimetric, *dissolved* H_2 indicator is required. In this paper we report the first example of such a H_2 indicator and demonstrate its use in screening for the activities of H_2-generating bacteria and measuring their total viable count (TVC).

2. Experimental

2.1 Materials

All chemicals and solvents were purchased from Merck (Gillingham, UK), unless stated otherwise. Double-distilled, deionized water was used to prepare all aqueous solutions. All gases were obtained from BOC (Surrey, UK) with the highest purity available. KWIK STIK stock cultures of the anaerobes *Escherichia coli* (*E. coli*, ATCC® 8739), *Klebsiella aerogenes* (*K. aerogenes*, ATCC® 13048), *Enterobacter cloacae* (*E. cloacae*, ATCC® 13047), and *Clostridium bifermentans* (*C. bifermentans*, ATCC® 638) and the aerobe *Pseudomonas putida* (*P. putida*, ATCC® 49128) were purchased from Microbiologics (St Cloud, Minnesota, USA). S2 of the SI file provides further background information regarding the bacteria. The 24-well plates used in this work were purchased from Corning (New York, USA) and had a well volume of 3.4 mL (internal diameter: 1.56 cm; maximum depth: 1.9 cm). The 15 mL plastic Falcon™ disposable sample tubes, with a proprietary O_2-sensitive fluorescent indicator set in its base, for making TVC measurements, were purchased from Oculer Ltd (Tipperary, Ireland). All other 15 mL plastic Falcon™ disposable sample tubes used in this work were obtained from Merck (Gillingham, UK). Details of the standard preparation of liquid and agar growth media used in this work are given in S3 of the SI. Details on making the stock dispersions of bacteria, and the plate counting method for determining the bacterial load in any dispersion, are given in S4 of the SI. All solutions for microbiological work were prepared fresh on the day. The units of the TVC values (or bacterial load) measured by the plate count method were CFU mL^{-1} and are reported as log(CFU mL^{-1}), with a typical error in log(CFU mL^{-1}) of *ca.* ± 0.1. The TVC of each inoculum was also confirmed using the plate count method which was always performed in triplicate.[22,23]

2.2 Preparation of the H_2 indicator

An aqueous platinum (Pt)-citrate colloid was prepared as described elsewhere,[24] by refluxing, for 4 h at 120 °C, a solution containing 30 mg of chloroplatinic acid, 30 mL of 1 wt% sodium citrate solution, and 120 mL of double distilled, deionized water. The resulting black Pt colloid was found to be stable for many months when stored under ambient conditions. A transmission electron micrograph (TEM) of the Pt colloidal particles is illustrated in S5 of the SI, revealing the colloid comprises strings of *ca.* 2.2 ± 0.5 nm Pt particles, of various length ranging from *ca.* 7 to 22 nm. A histogram of the distribution of Pt particle size is given in Fig. S2 in the SI, from which an average particle size of 2.2 ± 0.5 nm was derived.

The H_2 indicator ink, a precursor to the H_2 indicator, was prepared by first adding 0.135 g of hydroxyethyl cellulose (HEC) to 9 g of the black Pt colloid and stirring overnight. To this viscous solution were added, 0.9 g of glycerol, 25 mg polysorbate and 15 mg of the redox dye methylene blue (MB). The above H_2 indicator ink formulation was based on a photocatalyst activity indicator ink, *paii*, developed previously by this group,[25,26] comprising the same components, at the same levels, without the Pt colloidal particles. In both inks the different roles of the different components were as follows, (i) HEC, a polymer, used to encapsulate the other components in the dried ink *film*, (ii) MB, an established redox dye that provides a striking colour change when it is reduced to its *leuco* form, *leuco* methylene blue, LMB (iii) glycerol, a humectant, used to ensure the film doesn't dry out when stored, or used, in air, and which also functions as a plasticiser, to facilitate high gas diffusion into and out of the film, and (iv) polysorbate, a surfactant that reduces the surface energy of the ink and allows it to be spread evenly (and not reticulate) when coated on a low surface energy substrate, such as PET or Tyvek. The concentrations of each of these different components were optimised previously as a *paii* and retained in this work.[25] The maximum amount of Pt colloid was used in the H_2 indicator's formulation to ensure the fastest response.

The resulting mixture was then stirred for 30 minutes to ensure the dissolution of the ink ingredients. The final 'naked' H_2 indicator *film* was then produced by drawing down the indicator ink onto the inert substrate, white Tyvek® (Amazon, UK), using a K-bar #3 (RK Print Coat Instruments, Hertfordshire, UK). The K-bar deposited a wet indicator ink *film* of known thickness (24 μm) which was then allowed to dry in air (*ca.* 1 h) to produce a dry, blue-coloured, H_2-sensitive film, *ca.* 2 μm thick, as measured using a profilometer (Dektak3ST stylus-type profiler, Veeco, California, USA). Tyvek® was used as the inert support because it was highly gas permeable, due to its fibrous nature, and its white colour provided an excellent contrasting background to the blue-coloured H_2 ink film, to facilitate high quality digital photography.[21]

Because of the strict requirements of a *dissolved* H_2 indicator for monitoring *in situ* H_2 generating bacteria, see points (i)–(iii) in the Introduction, the above 'naked' H_2 indicator *film* was covered with a gas-permeable, ion-impermeable membrane (GPM). This GPM encapsulation was achieved by laminating the 'naked' H_2 indicator *film*, between two layers of thin (25 μm), low-density polyethylene (LDPE) sheet. Thus, a 7 × 7 mm square of the dried 'naked' H_2 ink on Tyvek® (a 'naked' H_2 indicator) was placed between two 12 × 12 mm square sheets of LDPE and the resulting 'sandwich' heated at 104 °C for 1 min using a heat press (VEVOR, London, UK). A photograph of the final (laminated) H_2 indicator, (henceforth, always referred to as the 'H_2 indicator') before (blue) and after (colourless) exposure to H_2 is illustrated in Fig. S3 in the SI. In this work the concentrations of gaseous and dissolved H_2 are always reported as a %, where 100% = 1 atm (gaseous) or, when used to saturate water at 25 °C, 100% = *ca.* 7.8×10^{-4} M (dissolved).

2.3 Other methods

A Cary 60 UV-Vis spectrophotometer (Agilent, Dublin, Ireland), was used to record all UV-Vis spectra. All digital photographs of the H_2 indicator were taken using a Canon EOS 700D digital camera (Canon Inc., London, UK), through the glass front window of the incubator (Heratherm™, Thermo Scientific, Massachuetts, USA), with a D65 daylight lamp (HiraLite 14 W full spectrum Daylight lamp, Amazon, UK) as the illumination source. The camera was placed 3 cm from the incubator window and 5 cm from the incubated Falcon tube, containing the solution under test, inside the incubator. Before taking photos, the custom white balance feature was activated on the camera using a white card, so that the camera locked into the colour temperature of the D65 daylight lamp from the light reflected from the card.

Each image of the H_2 indicator film was processed using digital colour analysis (DCA) for its red, green, and blue colour component space values (*i.e.*, RGB values) using the freely available processing software, Image J.[27] DCA analysis of the photographic image of the H_2 indicator allowed a value for its apparent absorbance, A', to be calculated, which can be shown to be directly proportional to the actual absorbance, A, of the indicator film at its absorption maximum, *ca.* 665 nm.[21] Further details regarding the DCA of the H_2 indicator film are given in S6 of the SI. A JEOL JEM 1400 transmission electron microscope (Hertfordshire, UK) was used to record transmission electron micrographs of the Pt colloid. A Pyroscience FireSting-O_2 fibre-optic oxygen meter (Aachen, Germany) was used to carry out all luminescence lifetime, τ, measurements of the Oculer O_2-sensitive indicator set in the base of a 15 mL Falcon™ tube. Note: As bacterial growth kinetics and the response of the H_2 sensor are temperature sensitive (*vide infra*), it was essential to carry out most of this work in a high quality incubator (±2 °C), a Heratherm™ incubator (Thermo Scientific, Massachusetts, USA), usually set at 37 °C.

3. Results and discussion

MB is known to be easily reduced to LMB, by many different reducing agents, such as sulfite and deprotonated glucose.[28,29] In contrast, MB can only be reduced by H_2 if there is also present a reduction catalyst, such as Pt.[30] Thus, the overall blue to colourless colour change observed for the H_2 indicator upon exposure to H_2, see Fig. S3 in SI, can be summarised by the following reaction equation,

$$MB_{blue} + H_2 \xrightarrow{Pt} LMB_{colourless} \quad (2)$$

The structures of MB and LMB are given in Fig. S4 of the SI.

Evidence for the above reaction was obtained by coating the H_2 indicator onto a quartz disc and recording its UV-Vis spectrum before and after exposure to H_2 gas, the results of which are illustrated in Fig. S5 in the SI. Before exposure, the blue-coloured H_2 indicator film exhibited an absorption spectrum

typical of the monomer and dimer forms of MB, with absorption peaks at, 292, 607 and 665 nm.[31,32] When bleached, by exposure to H_2, the UV-Vis spectrum of the now colourless film was that of LMB, with its characteristic absorption peak at 262 nm.[31,33]

In the absence of O_2, LMB is a very stable species but, in its presence, it is readily oxidised back to MB,

$$\mathrm{LMB} + 0.5\mathrm{O_2} \rightarrow \mathrm{MB} + \mathrm{H_2O} \quad (3)$$

Until here, there have been no reports of a *gaseous* and *dissolved* H_2 indicator *film* based on the above reactions, although Reichstein *et al.* have reported recently the synthesis of a *powder* comprising supraparticles of nanoparticulate silica and Pt, impregnated with MB, which react according to reactions (2) and (3) when exposed to *gaseous* H_2 and O_2, respectively.[34] Unfortunately, the latter colourimetric indicator is severely limited in application due to the need for a high, ambient relative humidity. Thus, no colour change is observed if the supraparticles are not also loaded with water and if dry gases are used.[34,35] Unfortunately, the above synthesised, H_2 *gas* colourimetric *powder* indicator cannot be used to measure *dissolved* H_2, due to issues of dye leaching. In contrast, the novel H_2 indicator described here has all the necessary features for such work as demonstrated by the results described below.

3.1 Characterisation of the H_2 indicator

As noted in the Experimental, in most of this work the H_2 indicator was monitored using photography coupled with DCA. Briefly, in DCA, the values of the red, green, and blue (RGB) components of the image are extracted and, for the blue-coloured (red absorbing) H_2 indicator, the associated value of its apparent absorbance, A', calculated *via* the following expression,

$$A' = \log\{255/\mathrm{RGB(red)}\} \quad (4)$$

where RGB(red) is the measured value of the red parameter in the RGB-analysed image of the indicator.[21] Previous work with numerous, differently coloured based indicators has demonstrated that in each case the value of A', as measured using photography coupled with DCA, is directly proportional to its actual absorbance, A, as measured using UV-Vis spectrophotometry.[21] This is also the case for the H_2 indicator, as demonstrated by a simple experiment in which the H_2 indicator was placed in an H_2 atmosphere to render it colourless *via* reaction (2), and then monitored simultaneously, using (i) photography/DCA and (ii) UV-Vis spectrophotometry, as the H_2 was allowed to exchange with ambient air, allowing the colourless indicator to return to its original blue colour, *via* reaction (3). The results of this work, *i.e.*, photographs and UV-Vis spectra of the indicator as a function of the H_2-air exchange time, and subsequent straight-line plot of A' (derived from DCA of the photographs) *vs.* A (from UV-Vis spectra) are illustrated in Fig. S6 in the SI. The latter plot, Fig. S6(c) in the SI, shows that when using the H_2 indicator, the parameter, A', which requires only an inexpensive camera to monitor, can substitute for A, and so, like A, can be taken as a direct measure of the concentration of MB, *i.e.*, [MB].

An initial study of the response (to H_2) and recovery (in O_2) kinetics of the H_2 indicator was carried out by placing it into a 1 cm cuvette (volume 4.18 mL) which was then sealed with a rubber septum. This cell was first flushed with Ar and its colour then monitored photographically as a function of time during the following sequence of different gas exposure steps, namely, (i) injection of 1 mL of 100% H_2, and left to stand for *ca.* 3.5 min, then (ii) flushing the cell with Ar, and left to stand for 25 min, and finally, (iii) injection of 1 mL of 100% O_2 and left to stand for 25 min. The photographic images of the H_2 indicator taken during steps (i)–(iii) are illustrated in Fig. 1(a)–(c), respectively. These photographs were subsequently analysed, using DCA and eqn (4), and yielded the plots of A' as a function of time, t, for the three different gas exposure steps, illustrated in Fig. 1(c). These results show that in step (i), the injected H_2, *ca.* 23.9%, quickly (within 3.5 min) reduces the MB in the H_2 indicator to LMB *via* reaction (2) and that, in the absence of O_2, *i.e.*, step (ii) with Ar as the inert headspace gas, the LMB form of the dye in the indicator film is stable, thereby highlighting the irreversible nature of reaction (2). In contrast, upon subsequent exposure of the reduced (colourless) H_2 indicator, to *ca.* 23.9% O_2, *i.e.*, step (iii), the indicator then slowly reverts to its original colour due to reaction (3). The 50% response time to H_2 and then O_2 in steps (1) and (iii) were 0.7 and 7.5 min, respectively.

This simple study reveals some notable kinetic features of the H_2-indicator, namely, (i) from the shapes of the decay and growth curves, the kinetics of reactions (2) and (3) are complex, (ii) the rate of reduction (of MB) is much greater than that of oxidation (of LMB), (iii) reaction (2) cannot be reversed by simply removing the H_2 present, and (iv) once in its colourless (LMB) form, the blue colour of the original H_2 indicator can be restored by exposing the indicator to O_2.

The same experiment was also carried out using a naked (no LDPE lamination layers) H_2 indicator, the results from which are illustrated in Fig. S8 in the SI. The 50% response time to H_2 and then O_2 were 0.3 and 6.8 min, respectively. Thus, the response time of the naked H_2 indicator was faster than that of the laminated H_2 indicator (0.7 min), which is not too surprising given the latter has a 50 μm layer of LDPE which acts as a barrier to diffusion. In contrast, the 50% colour recovery times of both the H_2 indicator and 'naked' H_2 indicator were similar (6.8 and 7.5 min, respectively) and much longer than the response times, which suggests that in both indicators the kinetics of colour recovery are dominated by the slow re-oxidation reaction (3), rather than simply the diffusion of O_2 from the gas phase into the indicator film.

Further work was carried out using this same set up, see Fig. S9 in SI, and showed that, despite the clearly complex nature of the kinetics, the reciprocal of the time taken for the indicator to lose (or regain) half its blue colouration, t_{50}, is directly proportional to the $\%H_2$ and $\%O_2$ in the headspace, and that, at 37 °C, the reduction process, reaction (2), is *ca.*

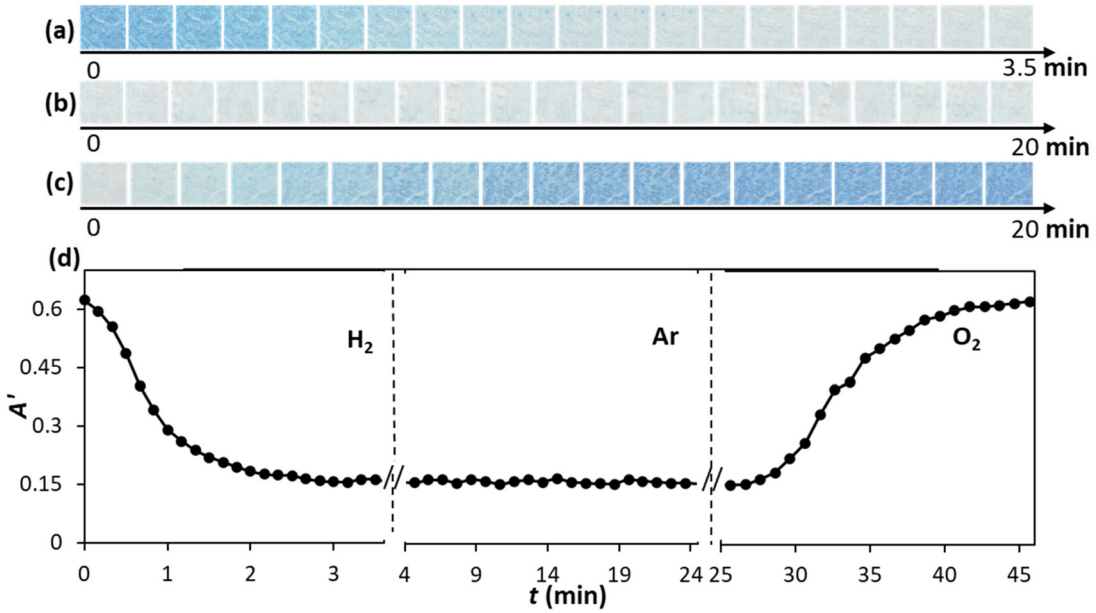

Fig. 1 (a–c) photographs of the H_2 indicator upon exposure to 23.9% H_2, then Ar and finally, 23.9% O_2 respectively. (d) *A′ vs.* time plots generated *via* DCA of the photographs in (a–c) and eqn (4). Temperature = 37 °C.

6×'s faster than reaction (3). The same MB reduction step was also carried out at 18 °C, which once again showed that $1/t_{50}$ was proportional to $\%H_2$, but with a gradient (0.013 min^{-1} $\%H_2^{-1}$) that was three times smaller than that found at 37 °C (0.039 min^{-1} $\%H_2^{-1}$), see Fig. S10 in the SI. This decrease in kinetics with decreasing temperature indicates an activation energy of *ca.* 43 kJ mol^{-1} for reaction (2).

Although not the primary focus of this paper, given that the H_2 indicator's colour can be restored in air, it was possible to generate a series of *A′ vs. t* peaks, by injecting different volumes of H_2 gas, V_{H_2}, into a stream of air, the heights of which are found to be proportional to V_{H_2}. The results of this very brief study are illustrated in Fig. S11 in the SI.

As the generation of H_2 by dark fermentation only occurs under anaerobic, or near anaerobic, conditions, it follows that in this work using the H_2 indicator, the only relevant colour changing process is reaction (2). Given $t_{50} \approx 1$ min when exposed to 23.9% H_2, and is roughly inversely proportional to the ambient level of H_2, see Fig. S9, it follows that it should take *ca.* 24 min to half-bleach if exposed to 1% H_2.

To demonstrate the efficacy of the H_2 indicator as a sensor for pure H_2, the same experiment, as used to generate the data in Fig. 1(a), was carried out using different levels of H_2, with the H_2 indicator's being restored by exposure to air. The results of this work, including the straight-line plot of $1/t_{50}$ *vs.* $\%H_2$, over the range 0.04 to 23.9%, are illustrated in Fig. S12 in the SI. The correlation coefficient of the line of best fit to the data, r, was 0.9932, the gradient ± standard deviation, $m \pm \sigma$, were 0.040 ± 0.002 min^{-1} $\%H_2^{-1}$ and the limit of detection ($3.3 \times \sigma/m$) was 0.16% H_2.

Finally, the long-term stability of the H_2 indicator in growth medium was demonstrated in a simple experiment in which the H_2-indicator was placed inside a 15 mL Falcon tube to which 10 mL of nutrient broth (NB), containing 3.97×10^{-4} M sodium sulfite, were then added. This solution represents the typical growth medium used in both the screening and TVC studies reported here. The Falcon tube was then sealed and incubated at 37 °C for 72 h and the indicator photographed every 4 h. The indicator stayed the same blue colour over the 72 h monitoring period and the DCA of recorded photographs of the indicator were used to produce the plot of *A′ vs.* incubation time, *t*, illustrated in Fig. S13 in the SI, from which an average value of $A' = 0.56 \pm 0.01$, was calculated. Additional work, using H_2 generating bacteria, showed that the response characteristics of the H_2 indicator were unchanged after this long-term exposure, *vide infra*. The results of this work suggest that the H_2 indicator is very stable and fully functional when placed in the bacterial growth medium for long periods of time, which is not surprising given it comprises a 'naked' H_2 indicator sealed between two layers of LDPE, where the latter ensures only gases, like H_2, can pass through to interact with the H_2 indicator ink film.

3.2 Screening H_2 bacterial activity

In a typical screening run, a H_2 indicator was fixed (using double sided tape), face (*i.e.*, blue side) down, to the bottom of each well, in the first two columns of a 6 rows × 4 columns, 24-well plate. In each well was placed 2.5 mL of growth medium, usually rendered anaerobic through the addition of 5 mg mL^{-1} sodium sulfite. In the first (the control) column, the growth medium was NOT inoculated with the bacterium under test, whereas in the second column it was inoculated. The *final* bacterial load (*i.e.*, TVC) in each of the 2.5 mL inoculated samples tested was *ca.* 10^7 CFU mL^{-1}, since these

samples were usually derived from a 10 mL anaerobic dispersion of the bacterium under test, by adding 1 mL of the overnight stock solution of bacterium (bacterial load *ca.* 10^8 CFU mL^{-1}) to 9 mL of growth medium. This 10 mL bacterial dispersion, and all paired blank/control solutions, also contained 50 mg of sodium sulfite, which rendered it anaerobic, as confirmed using an O_2 indicator to measure the $\%O_2$ present. Sulfite was not used in the *E. coli* and *P. putida aerobic* screening runs. In the *C. bifermentans* screening runs, as it was only possible to produce a stock dispersion of the bacterium with a load of *ca.* 10^7 CFU mL^{-1} (and not the usual 10^8 CFU mL^{-1}), only 2.5 mL of the neat stock dispersion, instead of the usual 10×'s diluted stock dispersion, was used to fill the well plate.

In this screening exercise, the bacteria tested were: *E. coli* (*anaerobic*), *K. aerogenes* (*anaerobic*), *E. cloacae* (*anaerobic*), *C. bifermentans* (*anaerobic*), *E. coli* (*aerobic*), and *P. putida* (*aerobic*). After the 2.5 mL, inoculated samples were added to the second column of 6 wells of the 24-well plate, the plate was sealed with a plate sealer (Greiner EASYseal clear, Stonehouse, United Kingdom), followed by the plate's lid and then incubated at 37 °C for 5 h. During this incubation period, the H_2 indicators at the bottom of the wells were collectively photographed at regular intervals from below the plate. A typical set of recorded photographs for incubation times of 0, 2.5 and 5.0 h are illustrated in Fig. 2 and show that, under *anaerobic* conditions (*i.e.*, with added sulfite to the growth medium), all the known H_2-generating bacteria, *i.e.*, *E. coli*, *K. aerogenes*, *E. cloacae* and *C. bifermentans*, generated sufficient H_2 to promote reaction (1) and, therefore, convert the MB to LMB.

In this simple, example screening trial, it *appears* the H_2 generating activities of the different bacteria were as follows, *E. coli* and *K. aerogenes* ≫ *E. cloacae* and *C. bifermentans*. This simple, one bacterial load, screening exercise is excellent for identifying, (i) the absence or presence of H_2-generating activity in a bacterium, (ii) the fastest (*i.e.*, most prompt) generating bacterium and (iii) the optimum conditions for H_2 production. However, it cannot provide a ready comparison of the different inherent rates of H_2 generation of the different bacteria due to many factors, not least of which is that each may exhibit very different lag phase times. Under the latter circumstances, an apparently slow H_2 producing bacterium, may actually have the highest intrinsic rate of H_2 evolution, but appear slow because it also exhibits a long lag phase under the employed screening conditions. In all the control (no bacteria) runs, the indicator did not change colour, showing that the H_2 indicator did not interact with the growth medium, nor was reduced by sodium sulfite, due to the LDPE GPM envelope. In this work, the screening system was only tested using non-photosynthetic bacteria but clearly has the potential to help identify and assess the activities of other H_2 generating microbial species, such as photosynthetic bacteria and algae.

As noted above, two other runs were carried out in which no sulfite was added to the growth medium, so that the bac-

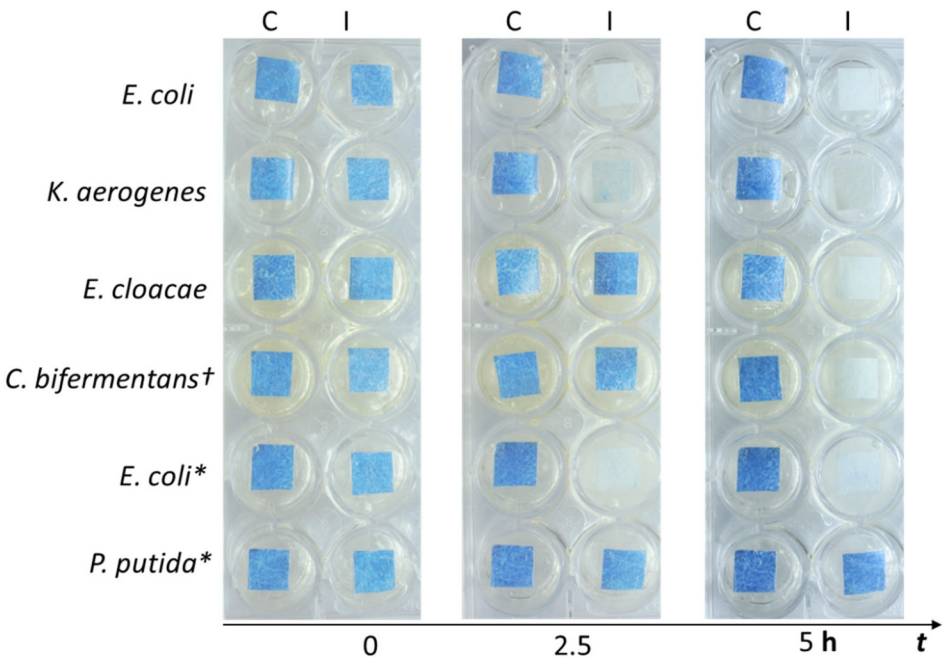

Fig. 2 Photographs (taken from below) of the first two columns of a 6 row, 24-well plate, in which each well contained a H_2 indicator set in its base, covered with 2.5 mL of a sodium sulfite-containing, and so O_2 free, growth medium. The photographs were recorded at 0, 2.5 and 5 h after the plate wells had been sealed and then placed in an incubator set at 37 °C. In the first column, *i.e.*, the control, marked 'C', the growth medium samples contained no bacteria, whereas in the second column, marked 'I', all were inoculated with *ca.* 10^7 CFU mL^{-1} of the bacterium under test. *In these two runs, no sulfite was added to the inoculated or control solutions, so that they were initially air-saturated.

teria tested, *E. coli* and *P. putida*, were initially under *aerobic* conditions. As noted earlier, dark fermentative H_2 production requires *anaerobic* conditions, and so, under *aerobic* conditions, *E. coli* (a facultative anaerobe) first consumes all the dissolved O_2 in the growth medium *via* the energy generating aerobic respiration process,

$$\text{Glucose} + 6O_2 \rightarrow 6CO_2 + 6H_2O. \quad (5)$$

Once the growth medium is rendered *anaerobic*, *E. coli* then generates energy for growth and, amongst other metabolites, H_2, *via* the dark fermentation of glucose, *e.g.*, reaction (1). At this point, the production of the latter is then picked up by the H_2 indicator, as illustrated by the results in Fig. 2. In contrast, *P. putida*, a strict aerobe, does not produce H_2, as evidenced by the photos of the H_2 indicator illustrated in Fig. 2.

To attempt a simple comparison of H_2 activities of different bacteria, all the inoculated plate wells contained approximately the same bacterial load (or TVC), *ca.* 10^7 CFU mL^{-1}. Clearly if the same growth medium was inoculated with the same bacterium, but with a lower bacterial load, the time taken the for the indicator to reach the half-way point in its colour change (from blue to colourless), t_{50}, would be longer. The latter feature offers up the possibility that the logarithm of the initial inoculum, always referred to here as $\log(N_o/(\text{CFU mL}^{-1}))$, and equivalent to log(TVC), might be simply related to t_{50}, and, consequently, could provide a simple, fast route for measuring the TVC of H_2-generating bacteria under anaerobic conditions. Such a method would be preferable to the traditional anaerobic plate counting method, PCM, which is slow (usually days), cumbersome and has a subjective element to it. The potential of using the H_2 to measure the TVC of H_2-generating bacteria, under anaerobic and aerobic conditions, is explored below.

3.3 Measurement of TVC under anaerobic conditions: *E. coli*

To place this work in context, it is worth outlining the principles and practice of the increasingly popular method of O_2 microrespiration for measuring the TVC of aerobes, *i.e.*, O_2 μR-TVC. This method involves the measurement of the TVC of aerobic and facultative anaerobic bacteria *via* the observed consumption of O_2 *via* reaction (5). O_2 μR-TVC is much faster (<24 h), simpler to use and less expensive than the traditional aerobic PCM.[36] In O_2 μR-TVC, the level of dissolved O_2 (or more usually the luminescence lifetime, τ, of the O_2 probe) in an inoculated growth medium is monitored as a function of incubation time, t. Thus, in a typical run, with an initial inoculum of a bacterium of N_o CFU mL^{-1}, an 'S' shaped τ *vs.* t profile is produced, from which a value for the incubation 'threshold' time, TT, is measured, where TT is defined as the value of the incubation time, t, at which τ is halfway through its transition from its initial (air-saturated) value, τ_{air}, to that when all the O_2 has been consumed, τ_o, *i.e.*, the value of t when $\tau = (\tau_{air} + \tau_o)/2$. Numerous studies show that for many relevant bacteria the log of the initial bacterial load of the inoculated growth medium, *i.e.*, $\log(N_o/(\text{CFU mL}^{-1}))$, is proportional to TT. Thus, in O_2 μR-TVC, a straight-line calibration plot of $\log(N_o/(\text{CFU mL}^{-1}))$ *vs.* TT is first generated for the bacterium under test, using samples of known bacterial load, and then used to calculate the value of TVC from the measured value of TT for any subsequent sample tested using O_2 μR-TVC. Such is the popularity of O_2 μR-TVC a simple commercial instrument, which allows high throughput TVC measurements based on O_2 μR-TVC, is now available.[37]

Clearly, O_2 μR-TVC cannot be used to assess the TVC of anaerobes or facultative anaerobes under *anaerobic* conditions, but, as a similar relationship, between respiration gas concentration (reactant or product) and incubation time, is likely to hold, it should be possible to use a H_2 indicator to measure TVC, and so establish H_2 μR-TVC as a method for measuring the TVC of H_2 producing, bacterial species.

In this work it is assumed that in a typical H_2 μR-TVC experiment, the measurable half-way colour change incubation time point, t_{50}, is, like TT, simply related to the initial inoculum, N_o. This assumption seems to be borne out by theory, see S8 in SI, assuming (i) the bacterial growth kinetics are described by the continuous logistic equation,[38]

$$dN(t)/dt = kN(t)[1 - (N(t)/N_{max})] \quad (6)$$

where N_{max} is the maximum number of bacteria the habitat can support and k is a proportionality constant that reflects how well the bacteria grows in the habitat, and (ii) the rate of H_2 production is proportional to $N(t)$. Theory, based on the above assumptions, predicts that in H_2 μR-TVC, like O_2 μR-TVC, a plot of $\log(N_o/(\text{CFU mL}^{-1}))$ *vs.* t_{50} will yield a straight line with a gradient that reflects the growth kinetics of the bacterium under test, see S8 in SI.

The following simple protocol was used to test the above prediction regarding H_2 μR-TVC. Thus, first the H_2 indicator was fixed to the bottom of a 15 mL Falcon® tube using double-sided tape, to which 9 mL of sterile, anaerobic (*i.e.*, containing 50 mg of sodium sulfite) growth medium were added (see S2 in SI). The indicator colour-change *vs.* incubation time run was then initiated by inoculating the 9 mL anaerobic growth medium with 1 mL of the bacterial dispersion under test, sealing the Falcon® tube, and then placing it in an incubator set at 37 °C, at which point the colour of the H_2 indicator was monitored photographically as a function of incubation time, t.

The above procedure was used to generate a $\log(N_o/(\text{CFU mL}^{-1}))$ *vs.* t_{50} calibration graph, based on a series of 1 mL inocula of the bacterium under test, of different bacterial load; the latter were derived from 10-fold diluted samples of the bacterial stock dispersion, and usually spanned the range 10^8–10^1 CFU mL^{-1}. Fig. 3 illustrates a typical set of results generated using the above H_2 μR-TVC protocol to generate a $\log(N_o/(\text{CFU mL}^{-1}))$ *vs.* t_{50} calibration graph with *E. coli* as the test bacterium. Any slight differences in colour in some of the photographic strips here and elsewhere in this paper and in the SI are due to slight differences in ambient light conditions as each strip was recorded at different times and on different

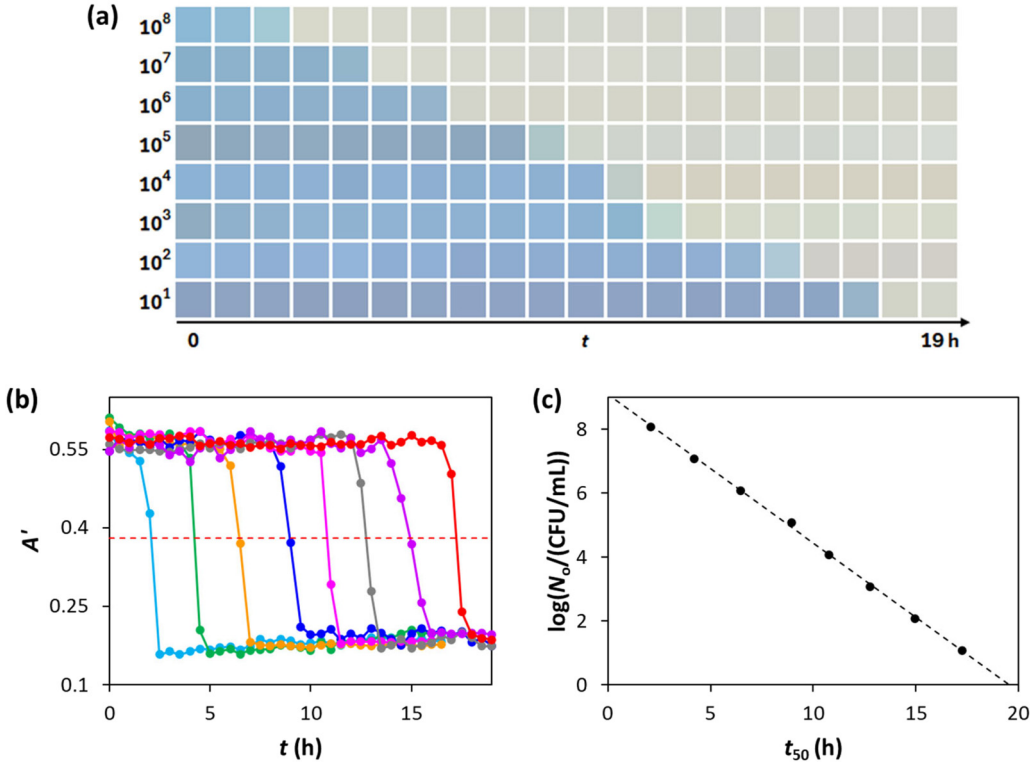

Fig. 3 (a) Photographic images of the H_2 indicator as a function of incubation time, t, in a typical set of H_2 μR-TVC runs, in which the 9 mL of anaerobic growth medium were inoculated with a 1 mL *E. coli* sample with a bacterial load spanning the range 10^8–10^1 CFU mL^{-1}. (b) A' *vs.* t reverse 'S' shaped profiles calculated from the photos illustrated in (a) using DCA and eqn (4), for initial inocula of (from left to right): 10^8, 10^7, 10^6, 10^5, 10^4, 10^3, 10^2 and 10^1 CFU mL^{-1}, respectively. The broken horizontal red line highlights the half-way colour change value, which is used to identify the value of t_{50} associated with each reverse 'S' shape profile/log(N_o/(CFU mL^{-1})) value. (c) Straight line, calibration graph plot of log(N_o/(CFU mL^{-1})) *vs.* t_{50} derived using data in (b). Incubation temperature: 37 °C.

days. These slight differences did not appear to generate inconsistent A' *vs.* t plots, as illustrated in Fig. 3(b).

All the photographic images generated in this experiment were analysed using DCA and eqn (4), to produce the series of A' *vs.* t reverse 'S' shaped curves illustrated in Fig. 3(b), from which, for each inoculum bacterial load, a value of t_{50} was determined and used in the production of the straight-line calibration plot of log(N_o/(CFU mL^{-1})) *vs.* t_{50} illustrated in Fig. 3(c). The results of this work confirm the theoretical prediction that H_2 μR-TVC can be used to generate the necessary straight-line calibration plot of log(N_o/(CFU mL^{-1})) *vs.* t_{50} that allows the method to measure the TVC (*i.e.*, the value of N_o/(CFU mL^{-1})) in any subsequent samples of the bacterium under test.

The gradient, m, and intercept, c, of the log(N_o/(CFU mL^{-1})) *vs.* t_{50} plot illustrated in Fig. 3(c) are given in Table 1.

It is also possible to extract from each of the A' *vs.* t profiles illustrated in Fig. 3(b), the time when the colour had only just started to drop (say by 10%, t_{10}, instead of 50% as in this work). This is of potential interest, given for each profile, $t_{10} < t_{50}$, and so would make the measurement of TVC faster. However, the very rapid colour change results in just a small (<20 min) difference between t_{10} and t_{50} and a marginal effect on analysis time. Despite this, it is worth noting that such a higher threshold would allow the method to be used for measuring the TVC of bacteria that generate much less H_2.

Table 1 Calculated line of best fit gradient (m) and intercept (c) values for straight line the log(N_o/(CFU mL^{-1})) *vs.* t_{50} H_2 μR-TVC plots for different bacterial species

	Log(N_o/(CFU mL^{-1})) *vs.* t_{50}		
Bacterium (CFU mL^{-1})	$m \pm \Delta m$	$c \pm \Delta c$	r^2
E. coli	−0.465 ± 0.013	9.08 ± 0.14	0.999
K. aerogenes	−0.521 ± 0.021	8.73 ± 0.20	0.990
E. cloacae	−0.669 ± 0.023	11.22 ± 0.23	0.994
C. bifermentans	−0.932 ± 0.013	11.13 ± 0.10	0.999
E. coli (aerobic)	−0.954 ± 0.027	9.82 ± 0.16	0.995

To demonstrate the high reproducibility of the H_2 indicator and the microrespirometry method, ten H_2 indicators, made on different days, were used to monitor the H_2 produced by a 1 mL inoculation of 10^4 CFU mL^{-1} *E. coli* in 9 mL of growth medium, as described above. The results of this work, a superimposed, series of near-identical A' *vs.* t profiles are illustrated in Fig. S14(a) of the SI, from which ten, very similar, values for t_{50} were determined, see Fig. S14(b), with an average value of 10.3 ± 0.3 h. The set of near identical, A' *vs.* t profiles illus-

trated in Fig. S14(a) and the low % standard deviation, 3%, in the t_{50} values, indicates a high level of reproducibility both in terms of the production of the H_2 indicator and the H_2 μR-TVC protocol.

A simple procedure was used to evaluate the effect, if any, on the response characteristics of the H_2 indicator after it had been exposed to the following different potential interfering species, ethanol, CO_2, methane, 2,3 butanediol, formic acid and H_2S. The test solution was water which was either saturated with 1% of the gas (CO_2, CH_4 and H_2S), or a 1 wt% aqueous solution, for the other, more soluble, potential interferents. The H_2 indicator was placed in the test solution for 30 min, before being removed, rinsed thoroughly and then evaluated in terms of its response characteristics, using the same simple microrespirometry method as described above. The photographs and associated A' *vs.* t profile recorded for each of the potential interferents are illustrated in Fig. S15(a) and (b), respectively, in the SI. The results show that, apart from for 1% H_2S, none of the potential interferents tested changed the response characteristics of the H_2 indicator.

The slower response of the H_2 indicator after exposure to 1% H_2S for 30 min, illustrated in Fig. S15 in the SI, is not unexpected, given sulfides are generally recognised as Pt catalyst poisons. Thus, although the H_2 indicator would be most likely able to detect H_2 generated by H_2 generating bacteria, it could not be used to assess the TVC if a significant (1%) level of H_2S was present. It follows that, when using H_2 μR-TVC to assess the TVC of a H_2 producing bacterium as in this work, the growth medium should not be conducive to H_2S generation and so not contain inorganic sulfur compounds (such as sulfate), nor sulfur-containing amino acids, such as cysteine. Since H_2S is a highly toxic gas, it is also not surprising that most reported H_2-producing bioreactors avoid its production by using a renewable biomass with a high content of carbohydrate, such as glucose, as noted in the Introduction. Note that 1% H_2S (10×'s the toxic level for humans) is not able to reduce MB to LMB in the H_2 indicator.

Previously, it was established that the colour of the H_2 indicator remained unchanged after being held for 72 h in the growth medium at 37 °C. The above simple microrespirometry test system was used to test the response features of the H_2 indicator before and after the 72 h incubation period and the results, illustrated in Fig. S16 in the SI, demonstrate that the indicator's response features remain unchanged with this prolonged exposure.

Finally, the same, simple microrespirometry test system is currently being used to evaluate the stability of the H_2 indicator when stored in a cool, dark place, with initial results proving promising as they show the indicator's response characteristics remain unchanged for at least 1 month, see Fig. S17 in the SI.

3.4 Measurement of TVC under anaerobic conditions: bacteria other than *E. coli*

The same study as carried out for *E. coli* and summarised by the results in Fig. 3, was carried out using the following different bacteria, *K. aerogenes*, *E. cloacae* and *C. bifermentans*, and the results of these studies are illustrated in S10 in the SI and the values of m and c, for the $\log(N_o/(\text{CFU mL}^{-1}))$ *vs.* t_{50} straight line calibration plots are also reported in Table 1. A quick inspection of the values of the gradients in Table 1, which are a measure of bacterial growth kinetics, suggests that *C. bifermentans* > *E. cloacae* > *K. aerogenes* > *E. coli*. Initially this order of growth kinetics might appear at odds with the screening results, where the H_2 generating activities of the different bacteria appear the very reverse, *i.e.*, *E. coli* and *K. aerogenes* ≫ *E. cloacae* and *C. bifermentans*. However, as noted earlier, the time at which H_2 appears in the screening will also depend upon the duration of any lag phase, caused by the bacterial cells adjusting to their new (fresh growth medium) environment; in contrast, the value of m should be indifferent to any lag time.

3.5 Measurement of TVC under aerobic conditions

H_2 μR-TVC is useful as it enables the measurement of the TVC (of H_2-generating bacteria) under *anaerobic* conditions, whereas O_2 μR-TVC is limited to measuring the TVC of aerobes and facultative anaerobes under *aerobic* conditions. However, this does not mean H_2 μR-TVC cannot be used to measure the TVC of H_2-generating bacteria under (initially at least) *aerobic* conditions. That it can do this was simply demonstrated by using the same protocol as before (see Section 3.3), but with no sodium sulfite in the growth medium, so that the inoculated samples were initially air saturated.

The results of such a study, using *E. coli* as the test bacterium, are illustrated in Fig. 4. The change in colour of the indicator with incubation time, illustrated in Fig. 4(a), shows that the H_2 is produced eventually, even when the solution is initially air-saturated. DCA analysis of the results in the latter figure, yield the reverse 'S' shaped A' *vs.* t plots associated with H_2 μR-TVC, see Fig. 4(b), from which the $\log(N_o/(\text{CFU mL}^{-1}))$ *vs.* t_{50} straight line calibration plot illustrated in Fig. 4(c) was generated, thereby demonstrating that H_2 μR-TVC can be used to measure the TVC of H_2 generating bacteria under initially aerobic conditions. It would appear quite likely that this would also apply to most, if not all, H_2 generating facultative anaerobes.

The values of m and c from the straight-line, $\log(N_o/(\text{CFU mL}^{-1}))$ *vs.* t_{50} plot illustrated in Fig. 4(c), are also given in Table 1, and suggest that the bacterial growth kinetics, as measured by the value of m, are twice as fast under *aerobic* conditions, compared to *anaerobic* conditions. This difference is perhaps not too surprising given that, under *aerobic* conditions, the major aerobic respiration process is the high energy-releasing reaction (5), $\Delta G = -2870$ kJ mol^{-1},[5] whereas under *anaerobic* conditions it is a dark fermentation process, such as reaction (1), which releases much less energy, $\Delta G = -48$ kJ mol^{-1}.[3]

At first it might appear unlikely that the H_2 indicator would change colour in an environment that was initially air saturated. However, during such a run, as noted earlier, the dissolved O_2 is rapidly consumed *via* the respiration process reac-

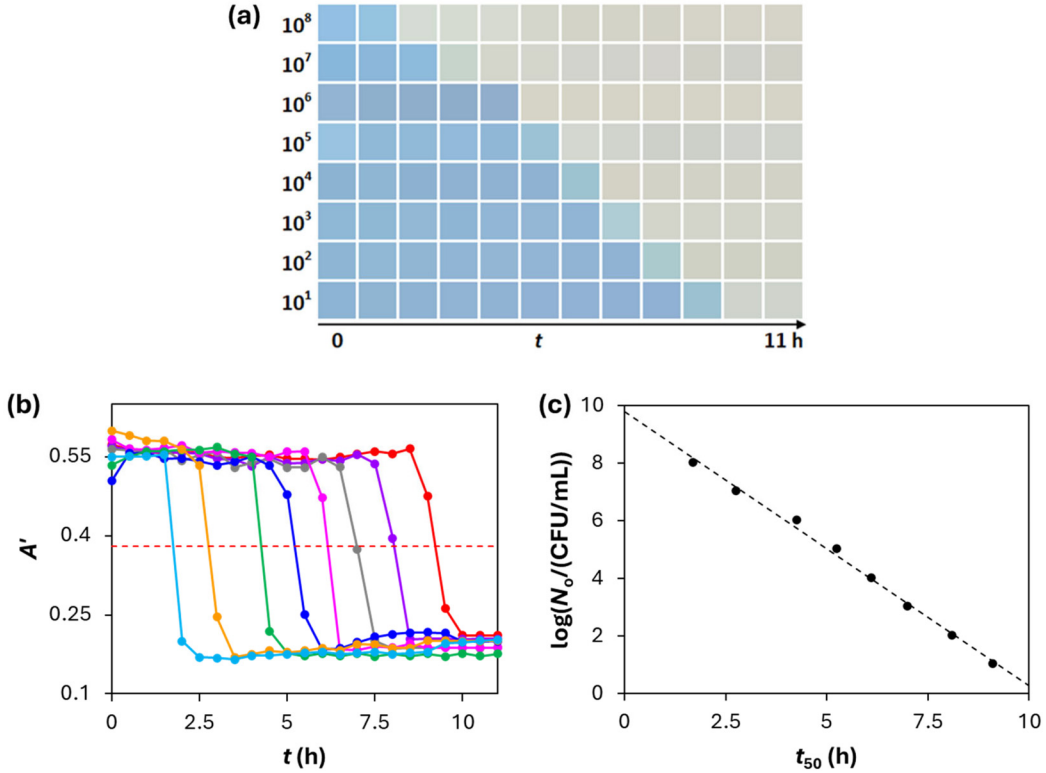

Fig. 4 (a) Photographic images of the H_2 indicator as a function of incubation time, *t*, in a typical set of H_2 μR-TVC runs, in which the 9 mL of air-saturated growth medium were inoculated with a 1 mL *E. coli* sample with a bacterial load spanning the range (from left to right) 10^8–10^1 CFU mL^{-1}. (b) *A′ vs. t* reverse 'S' shaped profiles calculated from the photos illustrated in (a) using DCA and eqn (4), for initial inocula of (from left to right): 10^8, 10^7, 10^6, 10^5, 10^4, 10^3, 10^2 and 10^1 CFU mL^{-1}, respectively. (c) Straight-line calibration graph plot of log(N_o/(CFU mL^{-1})) *vs.* t_{50} derived from the data in (b). Incubation temperature: 37 °C.

tion (5) and so, eventually the growth medium is rendered anaerobic, at which point the *E. coli* switches to the dark fermentative process, reaction (1), in which H_2 is generated, and so able to effect a change in colour of the H_2 indicator. This sequence of events was readily verified by carrying out a simple *aerobic* run, using a 1 mL inoculum of 10^4 CFU mL^{-1} of *E. coli*, in which both an O_2 and H_2 indictor were present. The results of this work, namely a plot of the luminescence lifetime, τ, of the O_2 indicator and the apparent absorbance, *A′*, of the H_2 indicator as a function of incubation time are illustrated in Fig. 5.

The results illustrated in Fig. 5 show that under *aerobic* conditions, the bacteria first consume all the dissolved O_2 in the system, with TT = 4.3 h, *via* reaction (5) and that, by *ca.* 5.5 h, the lifetime of the O_2 indicator is equal to τ_o, indicating *anaerobic* conditions prevail. It is at this point the H_2 indicator starts to respond to the presence of H_2, eventually producing the usual reverse 'S' shaped *A′ vs. t* curve with t_{50} = 6.2 h. Given the above results, it is perhaps not too surprising that subsequent work shows that, for the same inoculation run, the time difference between the half-way points in a H_2 indicator *A′ vs. t* plot (t_{50}) and the associated O_2 indicator τ *vs. t* plot (t_{TT}) is approximately the same (*ca.* 2 h), as in Fig. 5, over the range of *E. coli* inoculation range, 10^8–10^1 CFU mL^{-1}, see S11 in the SI. Consequently, the associated plots of log(N_o) *vs.* t_{50} and log(N_o) *vs.* t_{TT}, produces two good straight lines with very similar gradients as illustrated in Fig. S21(b) in the SI, separated by a time gap of *ca.* 2 h.

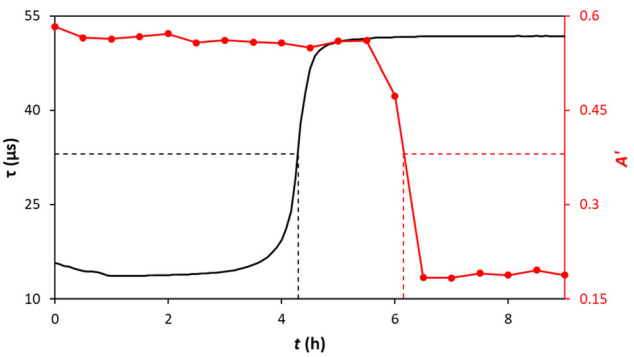

Fig. 5 Plot of the measured values of τ (black line, O_2 indicator) and *A′* (red line, H_2 indicator) as a function of incubation time, *t*, for a typical microrespirometry run in which 1 mL of growth medium containing 10^4 CFu mL^{-1} of *E. coli*, was used to inoculated 9 mL of air-saturated growth medium, incubated at 37 °C. The broken black line show the value of *t*, when τ reaches its midway transition point, *i.e.*, how the TT was determined. Similarly, the broken red line shows how the value of t_{50} was determined.

The linear calibration relationships obtained between log (TVC) and t_{50} mirror the behaviour of other micro-analytical sensing systems, in which gas-driven signal evolution follows predictable logistic or pseudo-first-order kinetics. A similar dependence of threshold-time parameters on analyte generation rates has been reported in microstructured detector platforms,[13,19] thereby reinforcing the general applicability of time-derived metrics for quantitative microbial analysis. By integrating this principle with a Pt-mediated H_2 indicator, the present study provides the first demonstration of a hydrogen-based analogue to O_2 μR-TVC.

4. Conclusions

A novel colourimetric H_2 indicator, comprising an intimate mixture of methylene blue (MB) and colloidal Pt encapsulated in a film of hydroxy ethyl cellulose and laminated between two thin sheets of LDPE, is easily prepared. This indicator can be used to screen by eye, or photographically, for H_2-generating microbial species in under anerobic or (initially) aerobic conditions. This indicator can be used to measure the TVC of H_2-generating bacteria, *via* a similar protocol as that used in the well-established, O_2 micro-respirometric methodology for measuring TVC, O_2 μR-TVC. This new method, H_2 μR-TVC, has the advantage over O_2 μR-TVC, in that it works primarily under *anaerobic* conditions and (initially) *aerobic* conditions. This simple H_2-indicator based screening process should prove invaluable to the many groups looking for, or generating new, H_2-generating microbial species to drive the efficient conversion of a renewable source, such as biomass, to H_2, as part of a future, environmentally friendly H_2 economy. Although it is likely this screening system could be extended to photosynthetic bacteria and algae, this would need to be demonstrated in a follow-up program of work. This work may also be of great interest to clinicians, interested in identifying the presence and TVC of H_2-generating pathogens, such as *E. coli* and *K. aerogenes*.

Author contributions

Lauren McDonnell Validation, formal analysis, investigation, writing-original draft. Christopher O'Rourke Conceptualization, methodology, validation, visualization. Michaella Watson Validation, formal analysis, investigation, writing – review and editing. Andrew Mills Conceptualization, writing – review & editing, supervision, project administration, funding acquisition.

Conflicts of interest

The authors declare that they have no known competing financial interests or personal relationships that could have appeared to influence the work reported in this paper.

Data availability

All data is provided in full in the results section of this paper and supplementary information (SI) accompanying this paper. Supplementary information is available. See DOI: https://doi.org/10.1039/d5an01221j.

Acknowledgements

This work was funded by the EPSRC (EP/T007575/1).

References

1 Hydrogen economy, https://en.wikipedia.org/wiki/Hydrogen_economy, (accessed January 2026).
2 X. Tao, Y. Zhao, S. Wang, C. Li and R. Li, Recent advances and perspectives for solar-driven water splitting using particulate photocatalysts, *Chem. Soc. Rev.*, 2022, **51**, 3561–3608.
3 J. Bartacek, J. Zabranska and P. N. L. Lens, Developments and constraints in fermentative hydrogen production, *Biofuels, Bioprod. Biorefin.*, 2007, **1**, 201–214.
4 D. Das and T. N. Veziroglu, Hydrogen production by biological processes: a survey of literature, *Int. J. Hydrogen Energy*, 2001, **26**, 13–28.
5 G. Gottschalk, *Bacterial Metabolism*, Springer-Verlag, New York, USA, 2nd edn, 1986.
6 D. Zhao, T. Wang and W. R. Heineman, Advances in H_2 sensors for bioanalytical applications, *TrAC, Trends Anal. Chem.*, 2016, **79**, 269–275.
7 Y. Zhou, W. Wei, H. Su and W. Wang, Sensitively fluorescent detection of H_2 with resazurin hydrogenation reactions catalyzed by Pd/C nanocomposites, *Inorg. Chem. Commun.*, 2019, **106**, 139–143.
8 A. Mills, A. Harriman and G. Porter, Membrane polarographic detectors for determination of hydrogen and oxygen produced by the photodissociation of water, *Anal. Chem.*, 1981, **53**, 1254–1257.
9 X. She, Y. Shen, J. Wang and C. Jin, Pd films on soft substrates: a visual, high-contrast and low-cost optical hydrogen sensor, *Light: Sci. Appl.*, 2019, **8**, 4.
10 J. Lee, H. Koo, S. Y. Kim, S. J. Kim and W. Lee, Electrostatic spray deposition of chemochromic WO_3-Pd sensor for hydrogen leakage detection at room temperature, *Sens. Actuators, B*, 2021, **327**, 128930.
11 D. Zhao, T. Wang, W. Hoagland, D. Benson, Z. Dong, S. Chen, D. T. Chou, D. Hong, J. Wu, P. N. Kumta and W. R. Heineman, Visual H_2 sensor for monitoring biodegradation of magnesium implants in vivo, *Acta Biomater.*, 2016, **45**, 399–409.
12 D. Fisher, M. Potter, P. Mandapati, M. W. Drover, S. Rondeau-Gagné and B. Mutus, Tetrazolium blue-based colorimetric sensor for hydrogen gas, *ACS Sustainable Chem. Eng.*, 2025, **13**, 15302–15310.

13 M. E. Smith, D. P. Rose, X. Cui, A. L. Stastny, P. Zhang and W. R. Heineman, A visual hydrogen sensor prototype for monitoring magnesium implant biodegradation, *Anal. Chem.*, 2021, **93**, 10487–10494.
14 A. K. Pathak, S. Verma, N. Sakda, C. Viphavakit, R. Chitaree and B. M. A. Rahman, Recent advances in optical hydrogen sensor including use of metal and metal alloys: a review, *Photonics*, 2023, **10**, 122.
15 K. Chen, D. Yuan and Y. Zhao, Review of optical hydrogen sensors based on metal hydrides: recent developments and challenges, *Opt. Laser Technol.*, 2021, **137**, 106808.
16 M. Ando, Recent advances in optochemical sensors for the detection of H_2, O_2, O_3, CO, CO_2 and H_2O in air, *TrAC, Trends Anal. Chem.*, 2006, **25**, 937–948.
17 Y. Shi, H. Xu, T. Liu, S. Zeb, Y. Nie, Y. Zhao, C. Qin and X. Jiang, Advanced development of metal oxide nanomaterials for H_2 gas sensing applications, *Mater. Adv.*, 2021, **2**, 1530–1569.
18 H. Liu, Z. Yang, L. Wang, P. Yu, Z. Kang, Q. Wu, C. Kuang and A. Yu, Gasochromic hydrogen sensors: fundamentals, recent advances, and perspectives, *Sens. Mater.*, 2023, **35**, 39–73.
19 P. S. Schrader, E. H. Burrows and R. L. Ely, High-throughput screening assay for biological hydrogen production, *Anal. Chem.*, 2008, **80**, 4014–4019.
20 J. Koo, T. Schnabel, S. Liong, N. H. Evitt and J. R. Swartz, High-throughput screening of catalytic H_2 production, *Angew. Chem., Int. Ed.*, 2017, **56**, 1012–1016.
21 D. Yusufu and A. Mills, Spectrophotometric and digital colour colourimetric (DCC) analysis of colour-based indicators, *Sens. Actuators, B*, 2018, **273**, 1187–1194.
22 ISO 4833-2, ISO 4833-2:2013, Microbiology of the food chain- horizontal method for the enumeration of microorganisms- part 2: colony count at 30 °C by the surface plating technique, International Organization for Standardization, Geneva, 2013.
23 M. Yamagata, Anaerobic plate count (spread and pour plate method), in *Laboratory Manual on Analytical Methods and Procedures for Fish and Fish Products*, ed. H. Hasegawa and K. Miwa, Marine Fisheries Research Department, Southeast Asian Fisheries Development Center, Singapore, 2nd edn, 1992, pp E9.1–E9.5.
24 A. Mills, Platinisation of semiconductor particles, *J. Chem. Soc., Chem. Commun.*, 1982, 367–368.
25 A. Mills, J. Hepburn and M. McFarlane, A novel, fast-responding, indicator ink for thin film photocatalytic surfaces, *ACS Appl. Mater. Interfaces*, 2009, **1**, 1163–1165.
26 Photocatalyst activity indicator ink, https://en.wikipedia.org/wiki/Photocatalyst_activity_indicator_ink, (accessed January 2026).
27 ImageJ, ImageJ, https://imagej.nih.gov/ij/index.html, (accessed January 2026).
28 A. Mills, K. Lawrie and M. McFarlane, Blue bottle light: lecture demonstrations of homogeneous and heterogeneous photo-induced electron transfer reactions, *Photochem. Photobiol. Sci.*, 2009, **8**, 421–425.
29 S. C. Engerer and A. G. Cook, The blue bottle reaction as a general chemistry experiment on reaction mechanisms, *J. Chem. Educ.*, 1999, **76**, 1519–1520.
30 T. Seo, R. Kurokawa and B. Sato, A convenient method for determining the concentration of hydrogen in water: use of methylene blue with colloidal platinum, *Med. Gas Res.*, 2012, **2**, 1.
31 N. R. de Tacconi, J. Carmona and K. Rajeshwar, Reversibility of photoelectrochromism at the TiO_2/methylene blue interface, *J. Electrochem. Soc.*, 1997, **144**, 2486–2490.
32 E. Braswell, Evidence for trimerization in aqueous solutions of methylene blue, *J. Phys. Chem.*, 1968, **72**, 2477–2483.
33 A. Mills and J. Wang, Photobleaching of methylene blue sensitised by TiO_2: an ambiguous system?, *J. Photochem. Photobiol., A*, 1999, **127**, 123–134.
34 J. Reichstein, P. Groppe, N. Stockinger, C. Cuadrado-Collados, M. Thommes, S. Wintzheimer and K. Mandel, Safety through visibility: tracing hydrogen in colors with highly customizable and flexibly applicable supraparticle additives, *Adv. Mater. Technol.*, 2024, **9**, 2400441.
35 J. Reichstein, S. Schötz, M. Macht, S. Maisel, N. Stockinger, C. C. Collados, K. Schubert, D. Blaumeiser, S. Wintzheimer, A. Görling, M. Thommes, D. Zahn, J. Libuda, T. Bauer and K. Mandel, Supraparticles for bare–eye H_2 indication and monitoring: design, working principle, and molecular mobility, *Adv. Funct. Mater.*, 2022, **32**, 2112379.
36 D. B. Papkovsky and J. P. Kerry, Oxygen sensor-based respirometry and the landscape of microbial testing methods as applicable to food and beverage matrices, *Sensors*, 2023, **23**, 4519.
37 Oculer, https://www.oculer.com/, (accessed January 2026).
38 M. G. Corradini and M. Peleg, Estimating non-isothermal bacterial growth in foods from isothermal experimental data, *J. Appl. Microbiol.*, 2005, **99**, 187–200.